Journal of Alloys and Compounds 488 (2009) 204–207

Contents lists available at ScienceDirect

Journal of Alloys and Compounds

journal homepage: www.elsevier.com/locate/jallcom

# Study of $LaCoO_3$ as a cathode catalyst for a membraneless direct borohydride fuel cell

Yan Liu, Jinfu Ma, Junhua Lai, Yongning Liu*

*State Key Laboratory for Mechanical Behavior of Materials, Xi'an Jiaotong University, Xi'an 710049, PR China*

ARTICLE INFO

*Article history:*
Received 12 July 2009
Received in revised form 14 August 2009
Accepted 15 August 2009
Available online 25 August 2009

*Keywords:*
Fuel cell
Cathode
Borohydride
$LaCoO_3$, Hydrogen storage alloy

ABSTRACT

In this paper, the perovskite-type oxide $LaCoO_3$ was studied as a cathode catalyst for use in a direct borohydride fuel cell (DBFC). The experimental results demonstrated that the $LaCoO_3$-catalysed cathode not only shows good electrocatalytic activity for oxygen reduction in alkaline solutions, but also shows good resistance to poisoning from $BH_4^-$ ions originating from the fuel during discharge performance. Based on this new type of catalyst, a membraneless fuel cell was designed with a hydrogen storage alloy used as the anode catalyst. The maximal current density of 220 mA cm$^{-2}$ and power density of 65 mW cm$^{-2}$ were obtained at ambient conditions.

## 1. Introduction

Fuel cell technologies have drawn significant attention for high efficiency in direct conversion of chemical energy into electricity energy, as well as environmental compatibility. Recently, certain liquid-type fuel cells have addressed the hydrogen supply and storage issues that arise in the proton exchange membrane fuel cell (PEMFC). The direct methanol fuel cell (DMFC) and direct borohydride fuel cell (DBFC) are liquid-fed designs. The DBFC has attracted recent research interest due to its high theoretical open cell voltage (OCV) of 1.64 V, high energy density (9300 mAh g$^{-1}$ for $NaBH_4$), more compact structure, and the possibility for use of non-precious metals as electrode catalysts [1–8].

In recent years, much effort has been directed to cathode catalysts for the DBFC [9–12]. For their high electrocatalytic activity and chemical stability, platinum, gold, or platinum-based catalysts have been widely investigated [13–16]. In addition to platinum, non-precious metal catalysts have been reported. Ag [17,18] was identified as a promising replacement for Pt and Pd catalysts for the DBFC, however, poor stability and weak resistance to borohydride influenced its performance as electrode [17]. $MnO_2$ [3,4,19] can eliminate degradation of the cathode arising from "$BH_4^-$ crossover", but the open circuit voltages of the $MnO_2$-catalysed cells were only about 0.8 V [4]. A cobalt polypyrrole carbon (Co-PPY-C) [20] was researched as the cathode catalyst and compared with Pt/C. However, the precious Nafion 117 membrane was used in the cell. Membraneless DBFCs were also designed by using metal phthalocyanines [21,22], which demonstrated good cell performance and excellent $BH_4^-$ tolerance.

Perovskite-type oxides are considered as promising catalysts for oxygen reduction owing to their high electrical conductivity and electrochemical properties, as well as good stability in alkaline solutions. There are many compounds similar to the natural perovskite $CaTiO_3$ and full of oxygen defects, a property that may accelerate transmission of oxygen [23].

Based on their advantageous catalytic properties, investigations on the use of perovskites in solid oxide fuel cells (SOFCs) [24,25] have been performed. It was thought that perovskite-type oxides could be used as electronic conductors and catalysts in the oxygen reduction reaction (ORR) in DBFCs as well as in the SOFCs. Our previous research focused on $LaNiO_3$ [26].

In this work, we prepared another perovskite-type oxide, $LaCoO_3$, as a cathode catalyst for a DBFC, which uses a hydrogen storage alloy as the anode catalyst. The catalyst structure was analyzed by X-ray diffraction (XRD) and scanning electron microscopy (SEM), and the cell performance and stability were studied by electrochemical methods.

## 2. Experimental

### 2.1. Materials and characterization

The $LaCoO_3$ perovskite was prepared by a sol–gel method. Lanthanum nitrate ($La(NO_3)_3$ $6H_2O$), cobalt nitrate ($Co(NO_3)_2$ $6H_2O$), citric acid ($C_6H_8O_7$ $H_2O$), and ammonia water ($NH_3$ $H_2O$) were used as the raw materials, all of analytical grade purity. According to the stoichiometric composition of the reactants, specified

---

* Corresponding author. Tel.: +86 29 8266 4602; fax: +86 29 8266 3453.
*E-mail address:* ynliu@mail.xjtu.edu.cn (Y. Liu).

0925-8388/$ – see front matter © 2009 Elsevier B.V. All rights reserved.
doi:10.1016/j.jallcom.2009.08.079

amounts of $La(NO_3)_3$ $6H_2O$ and $Co(NO_3)_2$ $6H_2O$ were first dissolved in deionized water and then an amount of $C_6H_8O_7$ $H_2O$ was added to the above solution. The amount of molar $C_6H_8O_7$ $H_2O$ was equal to the total molar metal nitrates in the solution. $NH_3$ $H_2O$ was slowly added to adjust the pH value of the solution to a range of 8–9 and to stabilize the nitrate–citrate solution. During this procedure, the solution was kept at a temperature of 70 °C and continuously stirred until a light-red gel was obtained; the precursor was produced from a subsequent drying process in a vacuum at 80 °C. The precursors were calcined at 600 °C, 700 °C, 800 °C, and 900 °C for 2 h in air to form $LaCoO_3$.

Crystalline structure characterization and morphology of the $LaCoO_3$ powder were investigated by X-ray diffractometer (D/MAX-3A, Japan) using Cu Ka radiation ($k$ = 0.154056 nm) and scanning electron microscopy (SEM, JEOL-S2700), respectively.

The anode catalyst, $MmNi_{3.55}Co_{0.75}Mn_{0.4}Al_{0.3}$ (where Mm denotes a Ce-rich mixed mischmetal composed of 50 wt.% Ce, 30 wt.% La, 5 wt.% Pr and 15 wt.% Nd) alloy, was prepared by inductive melting under argon atmosphere and the purity of all additive elements was over 99.9 wt.%.

### 2.2. Electrode preparation

The cathode electrode was of sandwich construction consisting of a gas diffusion layer, an active layer, and a current-accumulating matrix. The active layer was prepared by mechanically mixing 30 wt.% $LaCoO_3$ and 45 wt.% activated carbon with a 25 wt.% polytetrafluoroethylene (PTFE) emulsion. The slurry was pasted onto a Ni-foam (thickness = 1.7 mm, porosity > 95%). The gas diffusion layer was prepared by mixing 60 wt.% acetylene black (with surface area 2500 $m^2 g^{-1}$) and 40 wt.% PTFE with ethanol and pressing the mixture into a 0.3 mm thick film. Finally, the film was heat treated at 340 °C for 1 h. The three-layer gas electrode was finished by pressing the coated Ni-foam and the gas diffusion layer at 120 kgf $cm^{-2}$ into a 0.6 mm thick sheet.

A hydrogen storage alloy (HSA), $MmNi_{3.55}Co_{0.75}Mn_{0.4}Al_{0.3}$, powder (95 wt.%), was used as the anode catalyst. Acetylene black (2 wt.%) and cobalt monoxide (3 wt.%) were also added to improve the electrochemical activity and high-rate discharge ability of the alloy electrodes [27]. Then, the mixture was pasted onto a Ni-foam (thickness = 1.7 mm, porosity > 95%). After drying at 80 °C in a vacuum for 2 h, the electrode was pressed at 120 kgf $cm^{-2}$. Before measurement, the anode was soaked in a 6 M KOH and 0.4 M $KBH_4$ aqueous solution for 24 h for activation. The mass loading of $LaCoO_3$ in the cathode and HSA in the anode was 7.5 mg $cm^{-2}$ and 150 mg $cm^{-2}$, respectively.

### 2.3. Electrochemical measurements

Line sweep voltammetry (LSV) and discharge tests were employed to characterize the electrochemical performance of the cathode and anode using a computer controlled CHI600 Electrochemistry Workstation (Chenhua, Shanghai, China) with a conventional three-electrode configuration. The cathode and the anode served as the working electrodes. A Hg/HgO/6 M KOH electrode was as a reference electrode, and a Pt wire was used as a counter-electrode for polarization measurements. The 6 M KOH and 6 M KOH + 0.8 M $KBH_4$ solutions were used in the cathode and the anode polarization measurements, respectively. The performances of the DBFCs were measured using a battery testing system (from Neware Technology Limited, Shenzhen, China). The operation temperature for electrochemical tests was 25 °C.

## 3. Results and discussion

### 3.1. Physical characterization of $LaCoO_3$

During preparation of the catalysts, the proper calcination temperature is a key factor for formation of the materials. Therefore, we examined the influence of the calcination temperature on the physical characterization of $LaCoO_3$. Fig. 1 shows the XRD patterns of the $LaCoO_3$ powder after calcination in air for 2 h at 600 °C, 700 °C, 800 °C, and 900 °C. As seen in Fig. 1, looking at the XRD results of the amorphous precursor calcined at 600 °C and 700 °C, although the peak positions and their relative intensities are consistent with the standard powder diffraction patterns of a cubic perovskite-type $LaCoO_3$ phase (JCPDS, PDF code: 048-0123), some impure cobalt oxide peaks are found ($2\theta = 36.7°, 65.0°, 31.2°$), which suggests that at this temperature we could not obtain the single-phase catalyst. As the calcination temperature increased to 800 °C, the impure peaks of the phases almost disappear, indicating the formation of a complete crystal-phase structure. The phases of the powders calcined at 800 °C and 900 °C are the same, but the diffraction peaks of the powders calcined at 900 °C are sharper, showing better crystallinity of the powders.

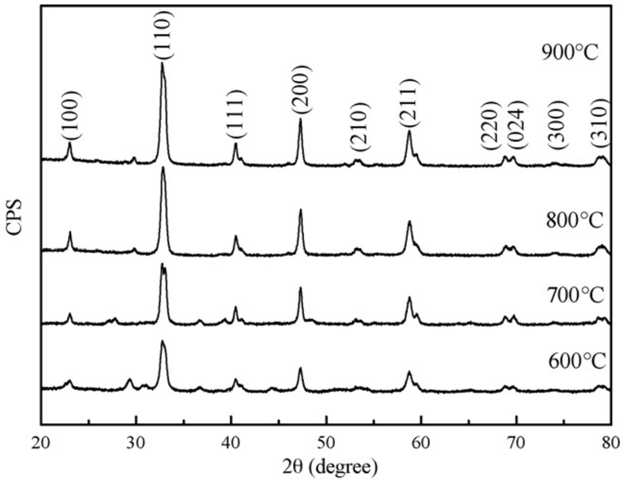

**Fig. 1.** XRD patterns of $LaCoO_3$ after calcination for 2 h in air at 600 °C, 700 °C, 800 °C, and 900 °C.

Fig. 2 shows SEM images of $LaCoO_3$ calcined at different temperatures. The particle sizes of the powder calcined at 600 °C and 700 °C are small and the surfaces are rough. For the sample calcined at 800 °C, not only is the particle size of the powder uniform, but the surface of the powder is also glabrous, showing the extensive crystallinity of the powder. Though the powder calcined at 900 °C also shows good crystallinity, agglomeration of the $LaCoO_3$ powder is obvious.

### 3.2. Influence of calcination temperature on cathode properties

Electrode polarization is one of the important properties for the cathode material in the DBFC. Fig. 3 shows the cathodic polarization curves of $LaCoO_3$ in order to confirm the best calcination temperature. It can be observed in Fig. 3 that the catalyst calcined at 800 °C demonstrates the minimum polarization and a current density of 220 mA $cm^{-2}$ at a cathode potential of −600 mV, thus showing the highest electrocatalytic activity for oxygen reduction in alkaline solution. The catalyst calcined at 700 °C had intermediate electrocatalytic activity. The $LaCoO_3$ calcined at 600 °C and 900 °C both shows low activity. The results may be attributed to the imperfect crystallization of the powder calcined at 600 °C and the obvious agglomeration of the particles calcined at 900 °C, as shown in Figs. 1 and 2.

### 3.3. Borohydride tolerance of cathode

To avoid using an expensive ion exchange membrane, the cathode electrocatalyst of the DBFC should have a good tolerance for borohydride. Fig. 4 illustrates the polarization curves of a $LaCoO_3$-catalysed cathode in 6 M KOH solution with or without the addition of 0.8 M $KBH_4$. As shown in Fig. 4, despite the small deviation in the OCV, the polarization curve of the $LaCoO_3$-catalysed cathode in the presence of $BH_4^-$ ions is approximately identical to that without $BH_4^-$ ions, indicating that the existence of $BH_4^-$ ions has basically no harmful effect on the discharge performances of the cathode. Due to its acceptable borohydride tolerance for the $BH_4^-$, we designed the DBFC system based on the $LaCoO_3$-catalysed cathode without using ion exchange membrane.

### 3.4. Cell performances

The performance of the cell at different discharge current densities is shown in Fig. 5. The working voltage of this DBFC decreases from 1.08 V to 0.22 V. With the growth of the discharge

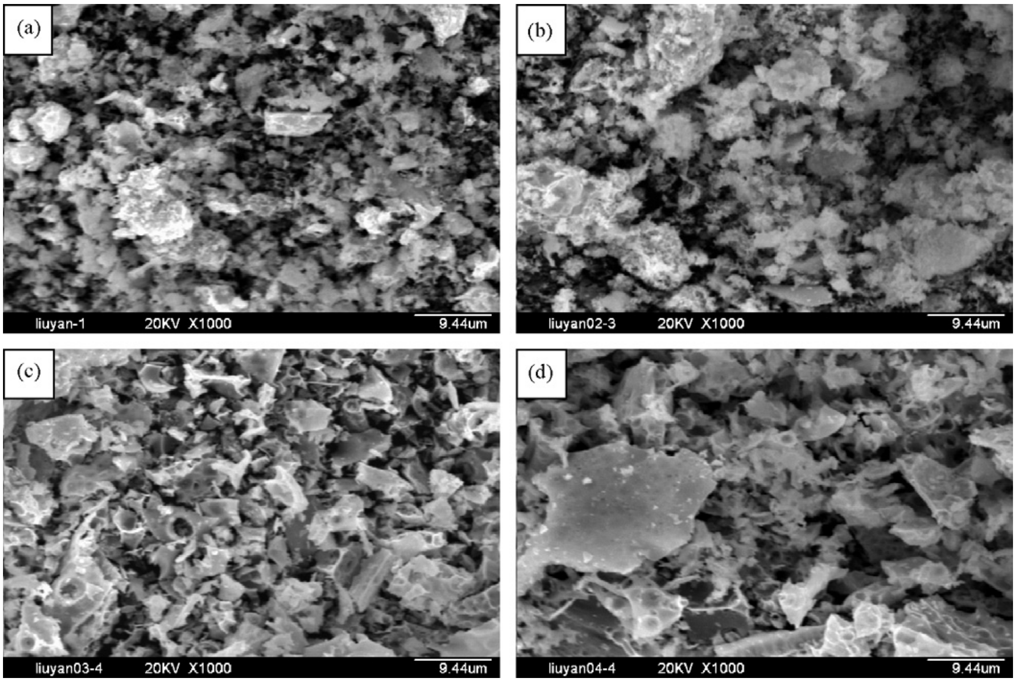

**Fig. 2.** SEM images of $LaCoO_3$ calcined at different temperatures: (a) 600 °C, (b) 700 °C, (c) 800 °C, and (d) 900 °C.

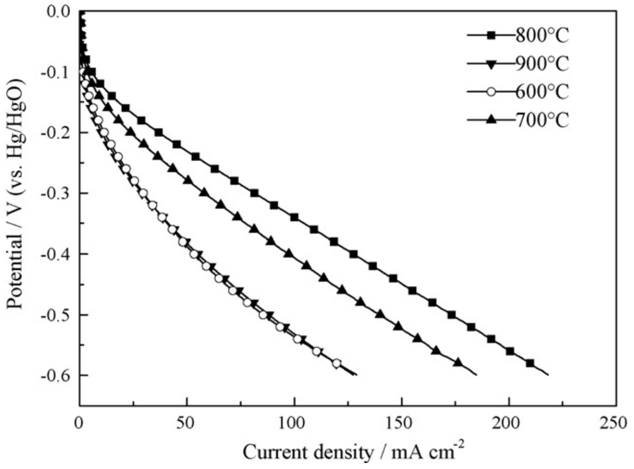

**Fig. 3.** Polarization curves of $LaCoO_3$ perovskite catalyst calcined at different temperatures (6 M KOH electrolyte solution; scan rate of 5 mV $s^{-1}$).

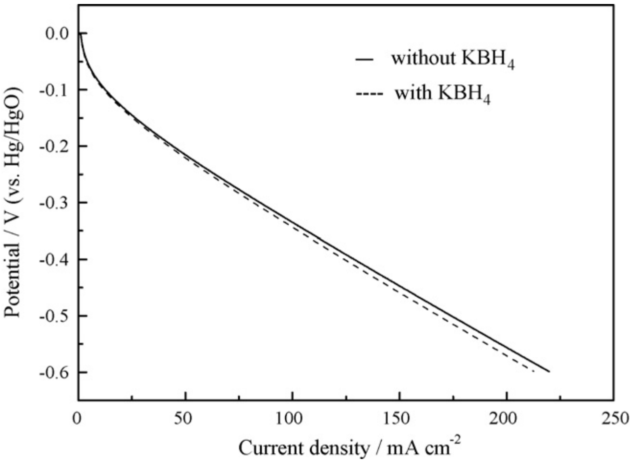

**Fig. 4.** Polarization curves of a $LaCoO_3$-catalysed air cathode in 6 M KOH solution with or without the addition of 0.8 M $KBH_4$ (scan rate: 5 mV $s^{-1}$).

current, the power density of this cell clearly increases at first and is then decreased. A maximum power density of 65 mW $cm^{-2}$ was obtained at 25 °C. Meanwhile, it can be seen from the steady-state polarization curve that the voltage and the current have almost a linear relationship suggesting there were no obviously activated polarization and concentration polarization except for ohmic polarization. The result also demonstrates that this type of electrode material shows good electrochemical performance.

### 3.5. Stability of the cell

It has been reported that cell performance stability was improved when Co-PPY-C was used as the cathode catalyst along with the reported Ag and Pt/C catalyst [20]. Fig. 6 gives a short-term stability comparison of the DBFC when using $LaCoO_3$ and Co-PPY-C as the cathode catalyst. As seen from Fig. 6, during a 50-h test, the cell performance stability was improved when using the

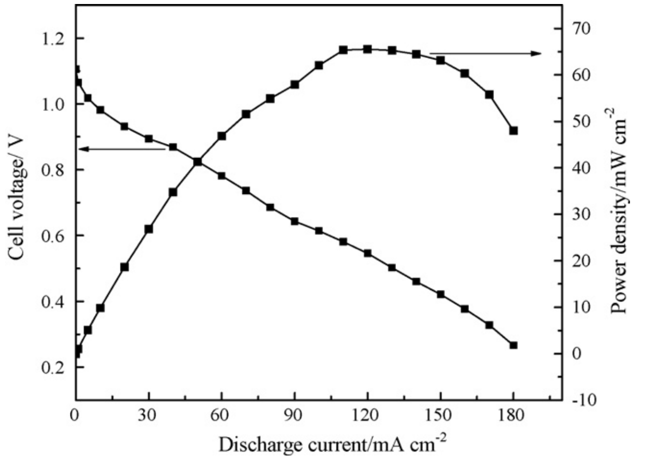

**Fig. 5.** Electrochemical performance of DBFC based on $LaCoO_3$ cathode and $AB_5$ alloy anode at different current densities.

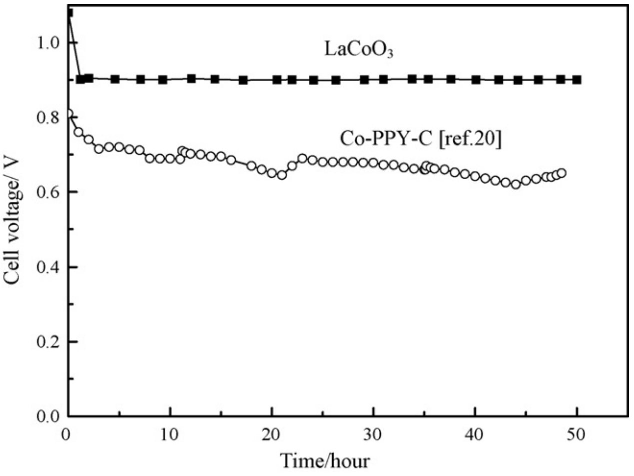

**Fig. 6.** Short-term stability of the DBFC using a $LaCoO_3$ cathode.

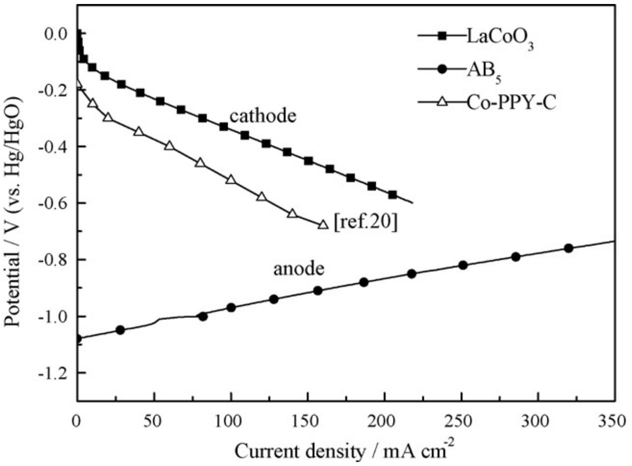

**Fig. 7.** Comparison of polarization between cathode and anode (scan rate: 5 mV $s^{-1}$).

$LaCoO_3$-catalysed cathode, indicating good stability for the DBFC system as designed.

### *3.6. Comparison of polarization between cathode and anode*

Comparison of the polarization curves for $LaCoO_3$ and Co-PPY-C used as the cathode catalyst and the polarization curve of the $AB_5$ anode are shown in Fig. 7. As this figure shows, the polarization of the Co-PPY-C-catalysed cathode [20] is much higher than that of the $LaCoO_3$ and the current density of the Co-PPY-C and $LaCoO_3$-catalysed cathode at a potential of −600 mV was 140 mA $cm^{-2}$ and 220 mA $cm^{-2}$, respectively. In addition, comparison of the potential variation between the cathode and anode shows clearly that the electrochemical dynamic performance of the anode is obviously superior to that of the cathode, suggesting the cathode causes a loss of cell voltage. For example, when the current density changes from 0 mA $cm^{-2}$ to 200 mA $cm^{-2}$, the cathode potential decreases from 0 V to −0.56 V and the anode potential is increased from −1.08 V to −0.87 V. The above analysis suggests that the cathode polarization significantly influences the cell output voltage. Therefore, in continuous applications, more attention should be paid to development of high efficiency non-precious metals or compounds as cathode electrode catalysts to further improve the cell performance.

## 4. Conclusion

In summary, using a sol–gel method, we prepared a simple low-cost $LaCoO_3$ catalyst. As a cathode catalyst, $LaCoO_3$ demonstrates acceptable activity for ORR and borohydride tolerance. A maximal current density of 220 mA $cm^{-2}$ and power density of 65 mW $cm^{-2}$ were obtained for this cell at ambient condition. Furthermore, the DBFC displayed good short-term stability during a 50 h continuous test. It is concluded that a perovskite-type oxide could be a potential candidate for cathode catalysts used in DBFCs.

## References

[1] Z.P. Li, B.H. Liu, K. Arai, S. Suda, J. Electrochem. Soc. 150 (2003) A868.
[2] R.K. Raman, N.A. Choudhury, A.K. Shukla, Electrochem. Solid State Lett. 7 (2004) A488.
[3] Y.G. Wang, Y.Y. Xia, Electrochem. Commun. 8 (2006) 1775.
[4] R.X. Feng, H. Dong, Y.D. Wang, X.P. Ai, Y.L. Cao, H.X. Yang, Electrochem. Commun. 7 (2005) 449.
[5] H. Cheng, K. Scott, J. Electroanal. Chem. 596 (2006) 117.
[6] Z.P. Li, B.H. Liu, K. Arai, S. Suda, J. Alloys Compd. 404 (2005) 648.
[7] A. Verma, S. Basu, J. Power Sources 145 (2005) 282.
[8] C. Ponce de Leon, F.C. Walsh, D. Pletcher, D.J. Browning, J.B. Lakeman, J. Power Sources 155 (2006) 172.
[9] E. Gyenge, M. Atwan, D. Northwood, J. Electrochem. Soc. 153 (2006) A150.
[10] M.H. Atwan, C.L.B. Macdonald, D.O. Northwood, E.L. Gyenge, J. Power Sources 158 (2006) 36.
[11] M.H. Atwan, D.O. Northwood, E.L. Gyenge, Int. J. Hydrogen Energy 30 (2005) 1323.
[12] B.H. Liu, S. Suda, J. Alloys Compd. 454 (2008) 280.
[13] B.H. Liu, Z.P. Li, S. Suda, J. Power Sources 175 (2008) 226.
[14] G.H. Miley, N. Luo, J. Mather, et al., J. Power Sources 165 (2007) 509.
[15] L.F. Gu, N. Luo, G.H. Miley, J. Power Sources 173 (2007) 77.
[16] C.P. de Leon, F.C. Walsh, A. Rose, et al., J. Power Sources 164 (2007) 441.
[17] B.H. Liu, S. Suda, J. Power Sources 164 (2007) 100.
[18] H. Cheng, K. Scott, K. Lovell, Fuel Cells 6 (2006) 367.
[19] A. Verma, A.K. Jha, S. Basu, J. Power Sources 141 (2005) 30.
[20] H.Y. Qin, Z.X. Liu, W.X. Yin, J.K. Zhu, Z.P. Li, J. Power Sources 185 (2008) 909.
[21] J.F. Ma, J. Wang, Y.N. Liu, J. Power Sources 172 (2007) 220.
[22] J.F. Ma, Y.N. Liu, P. Zhang, J. Wang, Electrochem. Commun. 10 (2008) 100.
[23] H.J.M. Lankhorst, B. meester, J. Electrochem. Soc. 144 (1997) 1261.
[24] Y. Tsvetkova, V. Kozhukharov, Mater. Des. 30 (2009) 206.
[25] A. Dutta, J. Mukhopadhyay, R.N. Basu, J. Eur. Ceram. Soc. 29 (2009) 2003.
[26] J. Ma, Y. Liu, Y. Liu, et al., Fuel Cells 8 (2008) 394.
[27] C. Iwakura, Y. Fukmto, M. Matsuoka, T. Kohno, K. Shinmou, J. Alloys Compd. 192 (1993) 152.